Phosphorylation Destabilizes the Amino-Terminal Domain of Enzyme I of the Escherichia c oli Phosphoenolpyruvate:Sugar Phosphotransferase System

ARTICLE *in* BIOCHEMISTRY · JUNE 1998

Impact Factor: 3.02 · DOI: 10.1021/bi980126x · Source: PubMed

Phosphorylation Destabilizes the Amino-Terminal Domain of Enzyme I of the *Escherichia coli* Phosphoenolpyruvate:Sugar Phosphotransferase System

Neil J. Nosworthy,[‡] Alan Peterkofsky,[§] Simone König,[||] Yeong-Jae Seok,[§,⊥] Roman H. Szczepanowski,[‡] and Ann Ginsburg*,[‡]

Section on Protein Chemistry, Laboratory of Biochemistry, Macromolecules Section, Laboratory of Biochemical Genetics, and Laboratory of Biophysical Chemistry, National Heart, Lung, and Blood Institute, National Institutes of Health, Bethesda, Maryland 20892

Received January 16, 1998; Revised Manuscript Received March 11, 1998

ABSTRACT: Thermal stabilities of enzyme I (63 562 M_r subunit), in the *Escherichia coli* phosphoenolpyruvate (PEP):sugar phosphotransferase system (PTS), and a cloned amino-terminal domain of enzyme I (EIN; 28 346 M_r) were investigated by differential scanning calorimetry (DSC) and far-UV circular dichroism (CD) at pH 7.5. EIN expressed in a Δ*pts E. coli* strain showed a single, reversible, two-state transition with T_m = 57 °C and an unfolding enthalpy of ∼140 kcal/mol. In contrast, monomeric EIN expressed in a wild-type strain (*pts*$^+$) had two endotherms with $T_m \cong 50$ and 57 °C and overall ΔH = 140 kcal/mol and was converted completely to the more stable form after five DSC scans from 10 to 75 °C (without changes in CD: ∼58% α-helices). Thermal conversion to a more stable form was correlated with dephosphorylation of EIN by mass spectral analysis. Dephospho-enzyme I (monomer ⇄ dimer) exhibited endotherms for C- and N-terminal domain unfolding with T_m = 41 and 54 °C, respectively. Thermal unfolding of the C-terminal domain occurred over a broad temperature range (∼30−50 °C), was scan rate- and concentration-dependent, coincident with a light scattering decrease and Trp residue exposure, and independent of phosphorylation. Reversible thermal unfolding of the nonphosphorylated N-terminal domain was more cooperative, occurring from 50 to 60 °C. DSC of partially phosphorylated enzyme I indicated that the amino-terminal domain was destabilized by phosphorylation (from T_m = 54 to ∼48 °C). A *decrease* in conformational stability of the amino-terminal domain of enzyme I produced by phosphorylation of the active-site His 189 has the physiological consequence of promoting phosphotransfer to the phosphocarrier protein, HPr.

The widespread bacterial phosphoenolpyruvate (PEP):sugar phosphotransferase system (PTS)[1] couples the translocation and phosphorylation of numerous sugars. The system is composed of two cytoplasmic proteins (enzyme I and HPr) that are used for all sugars as well as sugar-specific components known as enzymes II. Phosphoenolpyruvate is the phosphoryl donor in the Mg^{2+}-dependent autophosphorylation of enzyme I on histidine 189. Phospho-enzyme I reversibly transfers its phosphoryl group to histidine 15 of HPr (*1*). Phosphorylated HPr can donate its phosphoryl group to a variety of sugar-specific enzymes II, which ultimately phosphorylate specific sugars (*2*).

On the basis of proteolysis and fluorescence studies (*3*−*6*), it has been proposed that enzyme I from either *Escherichia coli* or *Salmonella typhimurium* is composed of a compact amino-terminal domain containing the active-site histidine (His 189) and a less structured, flexible carboxyl-terminal domain that is more susceptible to proteolysis. The amino-terminal domain of *E. coli* enzyme I extending from residues 1−258, with a C-terminal Arg added (EIN), has been cloned, expressed, and purified by Seok et al. (*7*), who showed that EIN can be phosphorylated reversibly in vitro by phospho-HPr but cannot be autophosphorylated by PEP, in agreement with the studies of LiCalsi et al. (*3*). X-ray crystallographic (*8*) and NMR solution (*9*) structures have recently been determined for EIN (1−258 + Arg). These show that EIN has an ellipsoidal shape approximately 78 Å long and 32 Å wide. The protein is composed of two subdomains: an α/β domain (residues 1−20 and 148−230) consisting of six β-strands and three helices and an α-domain (residues 33−143) consisting of four α-helices. The active-site His 189 is buried between the α and α/β domains and

* Address correspondence to this author at the National Institutes of Health, Building 3, Room 208, Bethesda, MD 20892-0340. Tel 301-496-1278; FAX 301-496-0599; e-mail aog@cu.nih.gov.

‡ Section on Protein Chemistry, Laboratory of Biochemistry.

§ Macromolecules Section, Laboratory of Biochemical Genetics.

|| Laboratory of Biophysical Chemistry.

⊥ Present address: Department of Microbiology, College of Natural Sciences, Seoul National University, Seoul 151-742, Korea.

[1] Abbreviations: PTS, phosphoenolpyruvate:sugar phosphotransferase system; PEP, phosphoenolpyruvate; EIN, amino-terminal domain (1−258 + Arg or 1−268 + Cys, containing either an introduced C-terminal Arg or Cys) of enzyme I (575 amino acid residues) of the phosphotransferase system; HPr, histidine-containing phosphocarrier protein of the phosphotransferase system; *pts*$^+$, wild-type strain of *Escherichia coli*; Δ*pts*, mutant strain of *Escherichia coli* with a deletion of the operon encoding genes expressing the phosphotransferase system proteins histidine-containing phosphocarrier protein, enzyme I, and enzyme IA^{glc}; 2-ME, 2-mercaptoethanol; DTT, dithiothreitol; DSC, differential scanning calorimetry; CD, circular dichroism; LS, light scattering.

S0006-2960(98)00126-3
Published on Web 04/23/1998

must rotate toward the solvent for interaction with phospho-HPr.

Calorimetric and circular dichroism studies reported here show that phosphorylation destabilizes the amino-terminal domain of enzyme I. While these studies were in progress, Chauvin et al. (*10*) reported on the cloning, expression, and characterization of a somewhat longer EIN construct (residues 1−268, with a C-terminal Cys added). Thermodynamic parameters were obtained for the reversible, two-state thermal unfolding of EIN (1−268 + Cys) in a nonphosphorylated form (*10*). Our results on the thermal unfolding of nonphosphorylated EIN (1−258 + Arg) agreed with those reported for EIN (1−268 + Cys). However, in vivo phosphorylation of EIN (1−258 + Arg) was found to decrease the T_m value for thermal unfolding from 57 to ∼50 °C. A similar phosphorylation-dependent destabilization of the amino terminal domain of full-length enzyme I also was observed. The physiological significance of the phosphorylation-dependent destabilization of enzyme I is discussed.

EXPERIMENTAL PROCEDURES

DNA Methods. A Δ(*ptsHIcrr*) mutant of strain GI698 (*11*) was constructed by P1 transduction (*12*) of the Km^R region from *E. coli* TP2811, in which the *pts* operon is replaced by the kanamycin resistance gene (*13*), into *E. coli* strain GI698. The wild-type (*11*) and Δ(*ptsHIcrr*) mutant of *E. coli* strain GI698 were transformed by electroporation with an *E. coli* Pulser (Bio-Rad) with the plasmids encoding enzyme I (pPR6) (*14*), EIN (1−258 + Arg) (pLP2) (*7*), and EIN (1−268 + Cys) (see below).

An expression vector for enzyme I, pPR6 (*14*), was used to construct a vector for the expression of EIN (1−268 + Cys). The 1660 bp *Bst*EII−*Bam*HI fragment encoding the C-terminal region of enzyme I was excised and replaced with a linker. The following two oligonucleotides were synthesized: (a) 5′-GTCACCAGTGTTAATAG-3′ and (b) 5′-GATCCTATTAACACTG-3′. Annealing of the two oligonucleotides resulted in the formation of a *Bst*EII and a *Bam*HI cohesive end, the codons for His267 and Gln268, and a Cys residue, followed by two stop codons. This linker was ligated to the linearized pPR6, yielding the plasmid encoding EIN (1−268 + Cys). The recombinant clone was verified by DNA sequencing.

Proteins. The transformants of strain GI698 were cultured under the conditions of Seok et al. (*7*) for hyperexpression of the proteins: enzyme I, 63 562 Da; EIN (1−258 + Arg), 28 346 Da; EIN (1−268 + Cys), 29 339 Da. The proteins were purified by a modification of a previous method (*7*) utilizing FPLC columns. Briefly, expression was induced by addition of L-tryptophan to a midlogarithmic phase culture (*11*), cells were harvested and resuspended in 10 mM Tris·HCl/100 mM NaCl, pH 7.5 (buffer A). The cells were ruptured by passage through a French pressure cell. After centrifugation, the supernatant was fractionated on a Mono Q HR10/10 column (Pharmacia) using a 0.1−0.5 M NaCl gradient in 10 mM Tris·HCl. Fractions were monitored by SDS−PAGE (*15*) using 4−20% gradient gels (Novex). Fractions containing the desired protein were equilibrated against buffer A and concentrated by centrifugation through Macrosep filters (3000 and 10 000 MW cutoff for EIN and enzyme I, respectively). The concentrates were applied to a Superose 12 column (1.6 × 50 cm) with buffer A as an eluent. Fractions containing the desired proteins that were homogeneous on SDS−PAGE were pooled.

Proteins were dialyzed at 4 °C overnight against several changes of 10 or 100 mM K-PO_4, pH 7.5, for EIN and 10 mM K-PO_4 with 2 mM 2-ME, pH 7.5, for enzyme I using Slide-A-Lyzer Cassettes (10 000 MW cutoff, Pierce). Dialyzed protein stock solutions (7−15 mg/mL) were stored at − 80 °C. Specific absorption coefficients used for spectrophotometric determinations of protein concentration were $A_{280nm,1cm} = 0.190$ mL/mg for EIN (see below) and $A_{280nm,1cm} = 0.40$ mL/mg for enzyme I (*16*).

Enzyme I was dephosphorylated by dialysis at 4 °C overnight against a buffer containing 10 mM K-PO_4, 10 mM pyruvate, 1 mM $MgCl_2$, and 2 mM 2-ME at pH 7.5 (*3*) followed by extensive dialysis against 10 mM K-PO_4 and 2 mM 2-ME, pH 7.5.

Circular Dichroism. CD measurements were performed with a Jasco J-710 spectrometer using 0.2 and 2 mm water-jacketed cylindrical cells. The temperature of cells was controlled by an external programmable water bath (Neslab RTE-110). Spectra were corrected for the solvent CD signal. CD spectra were normalized for protein concentration using values of 110.5 for enzyme I and 109.4 for EIN for the mean residue molecular weights. For determining secondary structure, far-UV spectra were the average of four accumulations taken at 10 nm/min. Secondary structural components were calculated by the method of Yang et al. (*17*) using software supplied by Jasco, Inc. For thermal denaturation studies, temperature was increased at a rate of 30 or 60 °C/h. CD data were analyzed either for a two-state or for two independent two-state reactions using the thermodynamic analysis program of Kirchhoff (*18*) and Origin software (MicroCal, Inc.) in the latter case.

Differential Scanning Calorimetry. DSC measurements were performed using MicroCal MC-2 and VP-DSC (*19*) calorimeters (MicroCal Inc., Northampton, MA) and a Nano-DSC (*20*) calorimeter (Calorimetry Sciences Corp., Provo, UT). Thermal denaturation of hen egg white lysozyme (0.06−3 mg/mL in 0.1 M glycine hydrochloride, pH 2.6) in the different DSC instruments at scan rates ≤ 45 °C/h gave previously measured thermodynamic parameters (*21*). The VP-DSC was run without feedback and equilibration times at 10 °C before or between scans with either the VP- or Nano-DSC was 10 min, whereas 1 h at 15 °C was allowed between scans with the MC-2 DSC. DSC data were corrected for instrument baselines and normalized for scan rate and protein concentration. Data were analyzed with Origin software (MicroCal, Inc.) and the program of Kirchhoff (*18*). Excess heat capacity (C_p) was expressed as kilocalories per kelvin per mole, where 1.000 cal = 4.184 J.

Analytical Ultracentrifugation. A Beckman Optima Model XL-A analytical ultracentrifuge equipped with a four-place AN-Ti rotor was used for sedimentation equilibrium experiments. A 12 mm cell equipped with a carbon-filled, 6-channel centerpiece and plane quartz windows was used. Increasing concentrations of each protein were loaded on the right (0.10 mL of enzyme I or 0.12 mL of EIN/channel) with 0.11 or 0.13 mL of reference buffer/channel, respectively (left). Dephospho-enzyme I (0.23, 0.45, and 0.90 mg/mL) was run at 10 000 rpm and 20.0 °C for 24 and 30 h and radial scans were made in 0.001 cm steps (step mode)

with 15 averages at 280 nm. Global, weighted fits of all data obtained for dephospho-enzyme I to a reversible association model for monomer ⇄ dimer gave $K_A = (1.8 \pm 0.1) \times 10^4$ (monomer)$^{-1}$ using software provided by Allen P. Minton (NIDDK/NIH) which can be downloaded from http://bbri.www.eri.harvard.edu/RASMB/rasmb.html. Sedimentation equilibrium experiments with partially phosphorylated or dephospho-enzyme I (*as above*) at 4 °C showed essentially only monomer (63 600 M_r), as has been reported previously by Waygood and Steeves (*22*). Sedimentation equilibrium experiments with nonphosphorylated or partially phosphorylated forms of EIN (0.4, 0.8, and 1.7 mg/mL) at 15 000−16 000 rpm at 4.0 and 20.0 °C for 26 or 31 h showed no association of monomers. Densities of dialysates were determined with an Anton Paar Model DMA 58 densitometer at 20.00 ± 0.01 °C. Partial specific volumes of 0.725 mL/g for EIN and enzyme I were calculated from amino acid compositions derived from DNA sequences (GenBank accession number J02796) and the values of Zamyatnin (*23*).

A Beckman Model XL-I in conjunction with the Perkin-Elmer Model 320 spectrophotometer was used to determine the specific absorption coefficient at 280 nm for nonphosphorylated EIN (*24*). After dialysis of EIN against 10 mM K-PO_4 (pH 7.5), the UV spectrum was measured: $A_{280nm,1cm} = 0.219$ after subtraction of the 340 nm absorbance (0.009). A portion of the solution of EIN from the spectrophotometer (0.13 mL) was placed on the right side of a 12 mm double sector capillary synthetic boundary cell centerpiece in a cell housing with sapphire windows and dialysate (0.41 mL) was put on the reference side. The cell was placed in a four-place AN-Ti rotor (at 20.0 °C) and immediately accelerated to 3 000 rpm and kept there until the temperature was stable at 20.0 °C (∼30 min). Then, the rotor speed was increased to 10 000 rpm to initiate boundary formation and in 2 000 rpm steps to 18 000 rpm until protein and solvent side menisci matched (10 min total time); the rotor then was decelerated to 3 000 rpm and 10 interference scans at 1 min intervals were collected. For 10 scans, the difference between the fringes in the plateau and solvent sides of the boundary (115 data points in both radial positions) gave 3.6568 ± 0.0016 fringes. A standard curve constructed for glutamine synthetase using the same instrument gave 3.191 ± 0.005 fringes (mg·mL)$^{-1}$ (M. Zolkiewski and A. Ginsburg, unpublished data). Thus, the EIN concentration was 1.15 ± 0.01 mg/mL and $A_{280nm,1cm} = 0.190 \pm 0.002$ mL/mg.

Fluorescence and Light Scattering. Fluorescence and light scattering measurements were conducted with a Aminco-Bowman Series 2 spectrometer. For changes in intrinsic tryptophanyl residue fluorescence with temperature, the excitation wavelength was 295 nm and emission was measured at the peak wavelength at 342 nm. For 90° light scattering, emission and excitation wavelengths were set at 360 nm. Temperature was controlled by a programmable Neslab RTE111 water bath and water-jacketed fluorescence cells were used. Temperature was measured by placing an Omega thermocouple into an identical water-jacketed fluorescence cell placed in line after the protein sample. Temperature ramp rates were monitored with a stopwatch. Progress curves for Trp exposure or light scattering changes were analyzed by the two-state thermodynamic analysis program of Kirchhoff (*18*).

Mass Spectrometry. Protein samples (10 μg of EIN in 10 μL of 10 mM K-PO_4) were diluted 1:1 with 5% acetic acid in 50:50 (v/v) methanol/water and subjected to on-line dialysis versus this solvent prior to loading into a Finnigan TSQ-700 mass spectrometer (FinniganMAT, San Jose, CA). The on-line dialysis was a modification of the method of Wu et al. (*25*) (S. König and H. M. Fales, unpublished results) using a single regenerated cellulose hollow fiber (13 000 MW cutoff); Fleaker hollow fiber concentrator from Spectrum Medical Industries, Inc. (Houston, TX). The mass spectra were obtained at ion source conditions of 200 °C (heated capillary) and 5.3 kV (needle). To minimize contributions from potassium adducts, the skimmer voltage was raised by 20 V and data were selected for lower charge states ($m/z > 1600$). Mass spectral data were deconvoluted using Finnigan software and smoothed with a fast Fourier transform using Origin software.

RESULTS

Thermal Unfolding of the Amino-Terminal Domain of Enzyme I. Markedly different DSC profiles were obtained for EIN (1−258 + Arg) when expressed and isolated from *E. coli* wild-type (*pts*$^+$) and Δ*pts* strains (Figures 1, panels A and B, respectively).

EIN produced in the wild-type strain and dialyzed against 10 mM K-PO_4, pH 7.5, had two endotherms of approximately equal areas with T_m values of ∼50 and 57 °C and overall $\Delta H_{cal} \cong 136$ kcal/mol (Figure 1A). Subsequent scans from 15 to 80 °C showed progressive decreases in the area of the lower temperature endotherm and corresponding increases in the area of the high-temperature endotherm. There was an isotemperature point at ∼54 °C for conversion of the protein to a more stable form during heating cycles in the calorimeter. Essentially the same results were obtained when EIN from the *pts*$^+$ strain was in 100 mM K-PO_4, 1 mM EDTA, and 0.5 mM DTT buffer, pH 7.5, but T_m values were increased to ∼54 and 59 °C with total areas of 138 and 140 kcal/mol for first and second DSC scans, respectively (data not shown). Sedimentation equilibrium analysis of EIN in either buffer indicated that the protein was a monomer of ∼28 000 M_r at 20 °C.

DSC profiles of EIN expressed and purified from the Δ*pts* strain GI698 showed only a single, reversible, and repeatable two-state transition at pH 7.5 (Figure 1B). The inset of Figure 1B shows the excellent fit of the data from the first DSC scan to a two-state model of unfolding. This result is similar to that reported by Chauvin et al. (*10*) for the somewhat longer EIN construct (1−268 + Cys) isolated from a different Δ*pts* strain. To exactly duplicate the results of Chauvin et al. (*10*), an EIN construct (1−268 + Cys) was introduced into the Δ*pts* strain GI698 (see Experimental Procedures), expressed, purified, and scanned by DSC (see Table 1 below).

The differences observed in DSC profiles for EIN isolated from *pts*$^+$ and Δ*pts* strains were not reflected by differences in overall secondary structure, as detected by CD measurements. Far-UV CD spectra measured at 20 °C for EIN (1−258 + Arg) isolated from either *pts*$^+$ or Δ*pts* strains were nearly the same (Figure 2A). Moreover, the secondary structure of either EIN form was recovered after cooling from 70 °C. The CD spectrum for EIN at 70 °C shown in Figure 2A demonstrated that unfolding was approximately complete at that temperature. An α-helical content of ∼58% for EIN

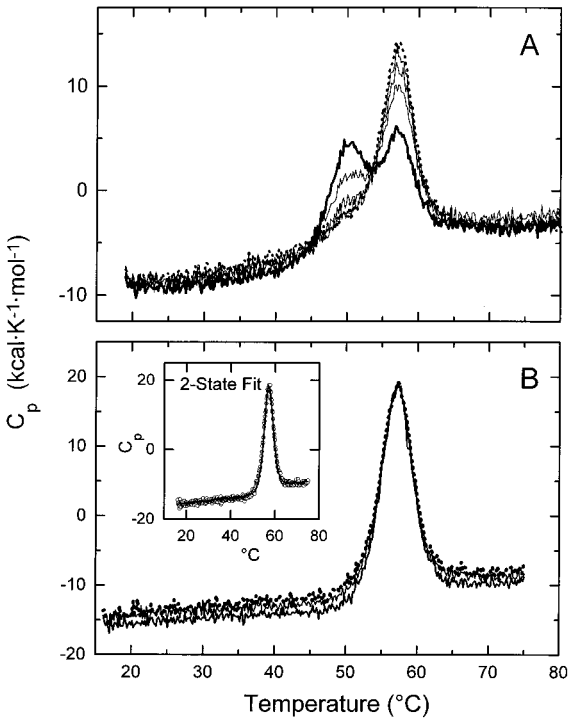

FIGURE 1: DSC profiles of EIN (1−258 + Arg) at scan rates of 60 °C/h in a MC-2 DSC with 1.0 mg/mL protein in 10 mM K-PO_4 (pH 7.5). (A) EIN was expressed and purified from a wild-type strain (*pts*$^+$), and five consecutive scans from 15 to 80 °C (with rapid cooling and equilibration at 15 °C for 1 h between scans) were performed: first scan (heavy line), total ΔH_{cal} = 136 kcal/mol; and with decreasing amplitude at 50 °C and increasing amplitude at 57 °C, second−fourth scans (thin lines); and fifth scan (···), total ΔH_{cal} = 130 kcal/mol. (B) EIN was expressed and purified from a Δ*pts* strain and three consecutive scans from 10 to 75 °C were performed as in panel A: first scan (heavy line), ΔH_{cal} = 139 kcal/mol; second scan (thin line); and third scan (···). The inset shows the fit (solid line) of the DSC data (open circles) from the first scan of B to a two-state unfolding model (with nonzero ΔC_p).

Table 1: Observed Thermodynamic Parameters for Thermal Unfolding of Nonphosphorylated EIN in 10 MM K-PO_4, pH 7.5[a]

EIN	concn (mg/mL)	T_m (°C)	ΔH (kcal/mol)	method	scan rate (°C/h)
(1−258 + Arg)	1.0	57.1	143	DSC[b]	60
(1−258 + Arg)	1.3	56.9	141	DSC[b]	60
(1−258 + Arg)	1.3	56.4	136	DSC[b]	30
(1−258 + Arg)	1.1	56.6	135	CD (222 nm)[c]	60
(1−258 + Arg)	0.95	56.5	132	CD (222 nm)[c]	30
(1−258 + Arg)	1.2	57.4	141	DSC[d]	60
(1−258 + Arg)	1.2	56.9	144	DSC[d]	30
(1−268 + Cys)	0.54	56.8	161	DSC[e]	60

[a] EIN was expressed and purified from a Δ*pts E. coli* strain. [b] An average ΔC_p value of 2.2 ± 0.5 kcal (K·mol)$^{-1}$ was estimated from pre- and posttransitional baseline extrapolations (*26*) using the model MC-2 from Micro-Cal, Inc. [c] The parameters T_m and ΔH were obtained from fitting the data to a two-state model of unfolding with ΔC_p = 2.7 kcal (K·mol)$^{-1}$ in the Exam program of Kirchhoff (*18*); see Figure 2B. [d] Using the VP-DSC from MicroCal, Inc. and the EXAM analysis program (*18*); ΔC_p = 2.7 kcal (K·mol)$^{-1}$. [e] Using the Nano-DSC from CSC, Inc. A ΔC_p value of 4.9 kcal (K·mol)$^{-1}$ was obtained by Chauvin et al. (*10*) for 1.9 mg/mL EIN(1−268 + Cys).

(1−258 + Arg) was estimated from the CD spectra at 20 °C (Figure 2A). This value approximated the proportion of α-helices deduced from X-ray crystallographic (*8*) and NMR solution (*9*) structures of EIN.

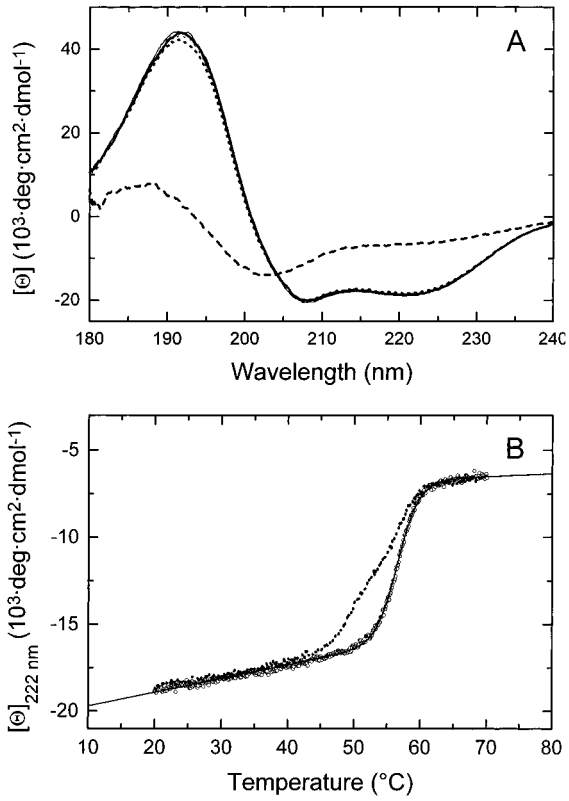

FIGURE 2: Thermally induced CD changes of EIN (1−258 + Arg). (A) Far-UV CD spectra at 20 °C are shown for EIN expressed in a *pts*$^+$ strain (heavy line; 0.93 mg/mL) and a Δ*pts* strain (thin line; 1.13 mg/mL) using a cell with 0.02 cm path length. Corresponding CD spectra recorded at 70 °C (- - -) and after cooling of heated samples to 20 °C (···) are shown. (B) Progress curves for temperature- induced CD changes at 222 nm are shown for EIN from a *pts*$^+$ (···) and from a Δ*pts* strain (open circles) together with the fit of the latter data to a two-state model of unfolding (solid line), taking into account sloping pre- and posttransitional baselines (*18*).

Thermally induced CD changes at 222 nm for EIN isolated from the *pts*$^+$ and Δ*pts* strains are shown in Figure 2B. EIN expressed in the *pts*$^+$ strain clearly exhibited two inflection points at approximately the same T_m values as observed in DSC experiments (Figure 1A). In contrast, thermally induced CD_{222nm} changes for EIN expressed in the Δ*pts* strain could be fitted perfectly to a two-state model of unfolding. This also agreed with the DSC results shown in Figure 1B. Thus, the conformational stability of EIN isolated from the different *E. coli* strains was reflected in both secondary structural and excess heat capacity measurements.

Mass spectral analysis of samples identical to those used for DSC studies are shown in Figure 3. The preparation of EIN isolated from the wild-type strain used for loading the DSC in the experiment of Figure 1A showed peaks of about equal intensities corresponding to 28 344 and 28 424 ± 2 Da. Since the calculated mass of EIN from the amino acid composition is equal to 28 346 Da, the addition of a -PO_3 adduct to His 189 would account for the 28 424 ± 2 Da peak in Figure 3 (with an apparent mass difference of ∼80 Da between observed species). After five consecutive DSC scans from 10 to 75 °C, the higher mass intensity peak (28 424 Da) was absent and the mass profile became identical to that for EIN isolated from the Δ*pts* strain, which was used for the DSC experiment of Figure 1B.

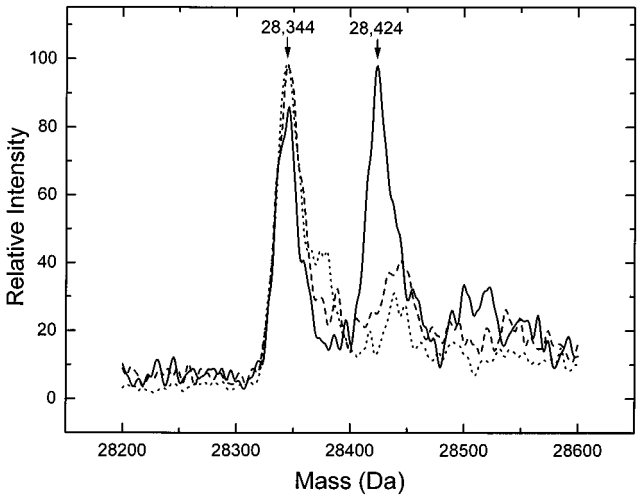

FIGURE 3: Mass spectral analysis of EIN (1−258 + Arg) samples from DSC studies. EIN expressed in a wild-type *pts*$^+$ strain that was used for loading the calorimeter in the experiment of Figure 1A showed peaks of approximately equal intensities corresponding to 28 344 and 28 424 Da forms (—). After the five consecutive scans shown in Figure 1A, the 28 424 Da form was not present and the mass profile became identical to that of a sample of EIN expressed and purified from the Δ*pts* strain (used for Figure 1B experiments), as shown by the dashed and dotted lines, respectively.

The mass spectral analyses were consistent with the interpretation that EIN (1−258 + Arg) was partially phosphorylated in vivo by phosphotransfer from phospho-HPr. Reversible phosphotransfer to EIN (1−258 + Arg) from phospho-HPr in vitro was demonstrated previously (*7*). Taken together, the results in Figures 1A, 2B, and 3 indicate that phosphorylation of His 189 destabilized the overall conformation of EIN. Moreover, the conversion of EIN to a more stable form during repeated heating cycles (Figure 1A) was correlated with hydrolysis of the phosphoryl group from His 189.

Table 1 summarizes thermodynamic parameters obtained for the reversible thermal unfolding of nonphosphorylated EIN at pH 7.5. Within experimental error, thermal unfolding was independent of scan rate. The T_m value from DSC of EIN (1−258 + Arg) was 56.9 ± 0.4 °C, which agrees with that obtained from CD_{222nm} data (Figure 2B); averaging DSC and CD data, $T_m = 56.8 \pm 0.4$ °C. The average ΔH_{cal} value of 141 ± 3 kcal/mol is comparable to the van't Hoff $\Delta H_{vH} = 134$ kcal/mol obtained from fitting CD data to a reversible, two-state unfolding model ($EIN_f \rightleftarrows EIN_u$). Thermodynamic parameters obtained by fitting CD_{222nm} data are reported in Table 1 for ΔC_p held constant at 2.7 kcal (K·mol)$^{-1}$. However, T_m and ΔH values were the same within experimental error when a 2-fold higher value of ΔC_p or $\Delta C_p = 0$ was assumed. The nonphosphorylated EIN construct (1−268 + Cys) had the same T_m value for thermal unfolding as EIN (1−258 + Arg). A somewhat greater ΔH_{cal} value of 5.4 cal/g for unfolding the longer EIN construct compared to that of 5.0 cal/g for EIN (1−258 + Arg) was obtained. The former value agrees with that reported by Chauvin et al. (*10*) for the same protein. The ΔC_p value measured for EIN (1−268 + Cys) [4.9 kcal (K·mol)$^{-1}$; *10*] also is larger than that measured for EIN (1−258 + Arg) [2.7 ± 0.2 kcal (K·mol)$^{-1}$; Table 1]. The larger denaturation enthalpy and higher ΔC_p values for EIN (1−268 + Cys) than measured for EIN (1−258 + Arg) may relate to the observation that

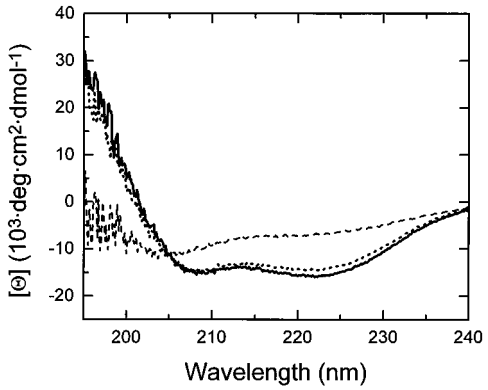

FIGURE 4: Far-UV circular dichroism spectra for dephospho-enzyme I (0.145 mg/mL; 0.2 cm path length) in 10 mM K-PO_4 and 2 mM 2-ME, pH 7.5. The solid and dotted lines show spectra recorded at 20 °C before and after heating at a rate of 30 °C/h to 70 °C, respectively. In a separate experiment, dephospho-enzyme I was heated at 30 °C/h to 70 °C and the CD spectrum was recorded (dashed line). The noise in the signal below 200 nm was due to the presence of the thiol reagent.

the C-terminal Cys residue of the longer EIN construct formed an intermolecular disulfide bond in the absence of a thiol reagent, as evidenced by bands corresponding to dimer and monomer in gel electrophoresis without reducing agent present.

Thermal Unfolding of Enzyme I. To study the unfolding of dephospho-enzyme I, the isolated, partially phosphorylated enzyme I was dephosphorylated (*3*; see Experimental Procedures). Enzyme I contains reactive cysteinyl residues in the C-terminal domain (*4*), which may be protected from oxidation by the addition of a thiol reagent. By conducting experiments at low concentrations of enzyme I (<0.2 mg/mL) in the presence of 2 mM 2-ME at low ionic strength, thermal transitions were reversible. Far UV-circular dichroism spectra of dephospho-enzyme I at pH 7.5 indicated that the native protein has ∼49% α-helix, ∼14% β-strand, and ∼27% random structures at 20 °C. At 70 °C, most of the secondary structure was disrupted (Figure 4). Upon cooling from 70 to 20 °C, the protein refolded to give nearly the same CD spectrum as recorded before heating (Figure 4). The thermally induced unfolding of dephospho-enzyme I was monitored by DSC, CD_{222nm}, and fluorescence changes due to tryptophanyl residue exposure at heating rates of 30 °C/h (Figure 5, panels A, B, and C, respectively). The two tryptophanyl residues of enzyme I are in the C-terminal domain and the T_m for Trp exposure (Figure 5C and Table 2) corresponded to the T_{max} of the lower temperature endotherm in DSC (Figure 5A). Thermally induced fluorescence changes due to Trp exposure gave a perfect fit to a model for a single two-state transition (Figure 5C). Changes in ellipticity at 222 nm occurred at both DSC endotherms (Figure 5B and Table 2). A satisfactory fit of DSC and CD_{222nm} data to a model of two independent, two-state transitions was obtained (Figure 5A,B). The lower temperature endotherm in Figure 5A occurred over a 20 °C range and was scan rate-dependent (Table 2), whereas the high-temperature endotherm was more cooperative (occurring over a 10 °C range) and was scan rate-independent.

Down-scans following up-scans and repeated scans from 10 to 70 °C of dephospho-enzyme I in the VP-DSC gave the same area of the high-temperature endotherm, whereas

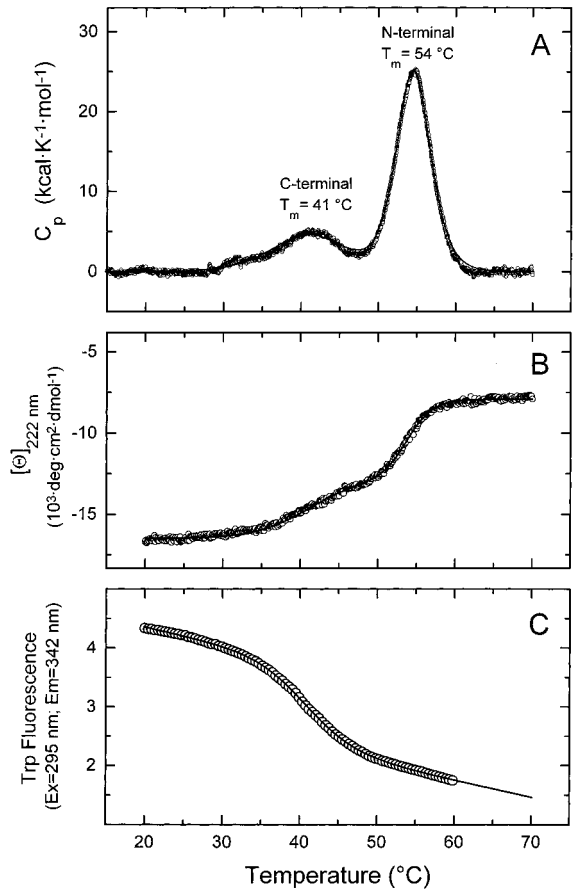

FIGURE 5: Thermal unfolding of dephosphorylated enzyme I. (A) Normalized DSC scan (after pre- and posttransitional baseline subtraction) of dephospho-enzyme I (0.138 mg/mL) in 10 mM K-PO_4 buffer, pH 7.5, obtained from 10 to 70 °C at a scan rate of 30 °C/h using the VP-DSC. A two two-state fit of the DSC data (open circles) to a model for two independent unfolding transitions (T_m = 41 and 54 °C) is shown by the solid line. (B) Thermally induced CD changes at 222 nm (open circles) and the fit to a model of two two-state, independent unfolding transitions (solid line); see Figure 4 and Table 2. (C) Thermally induced changes in the intrinsic tryptophanyl residue fluorescence (open circles); the fit to a single two-state model of unfolding with $\Delta C_p \cong 0$ is shown by the solid line. Measured CD and fluorescence changes (panels B and C) as a function of increasing temperature at a rate of ~33 °C/h for dephospho-enzyme I (0.145 mg/mL) in 10 mM K-PO_4 and 2 mM 2-ME buffer, pH 7.5, were reversible.

the low-temperature endotherm gradually disappeared. This may have been due to the absence of a thiol reagent in DSC experiments. When Trp exposure was measured in the fluorometer with 2 mM 2-ME present, the same transition was observed on reheating after cooling from 70 to 10 °C (Table 2) whereas in the absence of thiol reagent, Trp exposure was observed only during the first temperature increase. Nevertheless, ellipticity changes at 222 nm measured for dephospho-enzyme I in 10 mM 2-ME during a second heating from 20 to 60 °C at 30 °C/h occurred at ~3 °C higher temperature than observed for T_m^1 on a first heating whereas T_m^2 was the same (data not shown). This suggests that some cross-linking of the C-terminal domain occurred during heating even in the presence of excess 2-ME.

Thermodynamic parameters for the thermal unfolding of dephospho-enzyme I at pH 7.5 are summarized in Table 2. Enthalpy and T_m values were obtained from fitting DSC, CD_{222nm}, and fluorescence data at the indicated scan rates to

Table 2: Summary of Thermodynamic Parameters for Thermal Unfolding of Dephospho-enzyme I in 10 MM K-PO_4, pH 7.5[a]

enzyme I concn (mg/mL)	T_m^1 (°C)	T_m^2 (°C)	ΔH^1 (kcal/mol)	ΔH^2 (kcal/mol)	method	scan rate (°C/h)
0.150	42.8	55.2	46.4	141	VP-DSC	60
0.138	41.2[b]	54.5[b]	58.4[b]	145[b]	VP-DSC	30
0.425	41.5	54.5	75.1	141	VP-DSC	30
0.145	40.1	54.1	55.8	154	VP-DSC	10
0.150[c]	39.9	53.9	62.1	118	CD (222 nm)	60
0.145[c]	41.2	53.8	56.2	129	CD (222 nm)	30
0.138	40.5	nt[d]	59.0	nt[d]	Trp fluor	64
0.148[c]	41.1	nt	54.3	nt	Trp fluor	33
	40.9		61.2		2nd fluor scan	33
0.150	39.7	nt	55.6	nt	Trp fluor	33
0.138[e]	39.2	nt	~80	nt	90° LS	64
0.138[c,f]	41.8	nt	56.3	nt	Trp fluor	64
0.143[c,f]	40.7	nt	61.8	nt	Trp fluor	33

[a] Enzyme I was isolated from the Δ*pts E. coli* strain and then a stock solution (~15 mg/mL) was dialyzed first against pyruvate/$MgCl_2$ in the presence of 2 mM 2-ME at pH 7.5 to remove covalently bound phosphate (see Experimental Procedures) and then against 10 mM K-PO_4 and 2 mM 2-ME, pH 7, and stored at −80 °C. Dilutions of the stock solution of dephospho-enzyme I (~7.5 mg/mL) were made just prior to measurements. Thermodynamic parameters were obtained by fitting DSC and CD to a model for two independent two-state transitions or by fitting fluorescence data (ex = 295 nm; em = 342 nm) and 90° LS (360/360 nm) data to a model for a single two-state unfolding reaction (see Figure 5). [b] Parameters from the fit in Figure 5A. [c] With 2 mM 2-ME added to the dilution buffer (10 mM K-PO_4, pH 7.5).[d] nt, no transition was observed. [e] The amplitude of the LS decrease was small; ~4% expected for dimer → 2 monomers at this concentration of protein from the value of $K_A = 1.7 \times 10^4$ (M monomer)$^{-1}$ obtained from sedimentation equilibrium experiments at 20 °C. [f] Partially phosphorylated enzyme I, as isolated from the Δ*pts* strain (see Figure 6).

models for reversible, independent, two-state unfolding transitions. In addition, a small light scattering decrease that occurred at $T_m \cong 39$ °C was analyzed by a two-state model. The LS decrease reflected the dissociation of a small amount of enzyme I dimer present. The dimerization constant determined by sedimentation equilibrium for dephospho-enzyme I at 20 °C indicates that < 5% of the protein exists as a dimer at 0.15 mg/mL concentration. The dimerization of enzyme I has been observed to be temperature-dependent (*22*, *27*), but even if K_A increases 10-fold from 20 to 30 °C, the amount of dimer would be less than 10% at 0.15 mg/mL. A light scattering increase was not observed as the protein was heated from 20 to 30 °C and the decrease in LS observed at higher temperatures indicates that unfolding of the C-terminal domain destabilized any dimer present. This is not surprising since the C-terminal domain of enzyme I is necessary for dimer formation (*6*, *10*).

The area of the low-temperature endotherm (Figure 5A) corresponding to the unfolding of the C-terminal domain of enzyme I at pH 7.5 and 0.15 mg/mL (ΔH^1 in Table 2) is ~50% of that previously reported by LiCalsi et al. (*3*) for a 10-fold higher concentration (and higher ionic strength). When enzyme I was scanned at 3-fold higher concentration, ΔH^1 increased from ~57 to 75 kcal/mol (Table 2). This suggests that dimerization stabilizes additional structures in the C-terminal domain of enzyme I that unfold at ~41 °C. LiCalsi et al. (*3*) also reported T_m values of 47.6 and 54.9 °C for dephospho-enzyme I in 100 mM K-PO_4, 1 mM EDTA, and 0.5 mM DTT at pH 7.5 at a scan rate of 60 °C/h. DSC studies of the G338D mutant of enzyme I (1.85

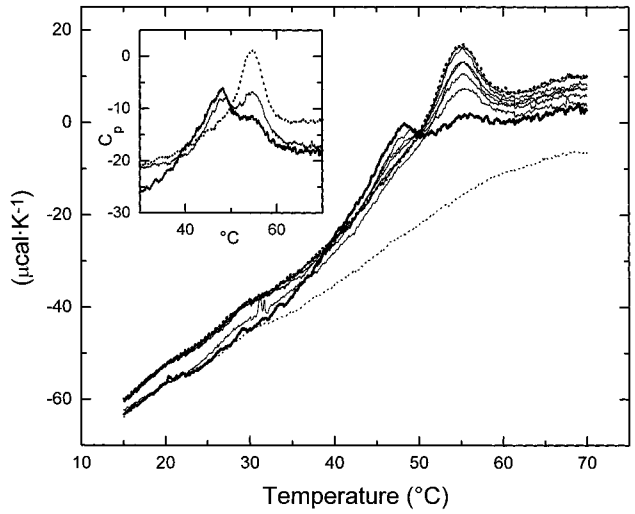

FIGURE 6: Consecutive DSC scans of partially phosphorylated enzyme I. Raw DSC data for the buffer baseline after offsetting to the initial protein signal (···) and eight consecutive scans from 10 to 70 °C for partially phosphorylated enzyme I isolated from a Δ*pts* strain are shown. The protein (0.150 mg/mL in 10 mM K-PO_4 buffer, pH 7.5) and dialysate were heated at scan rates of 60 °C/h (with 10 min of equilibration at 10 °C between scans) in the VP-DSC. Scans 1−8 showed a progressive increase in the endotherm area (and peak amplitude) with $T_m \cong 54$ °C and a corresponding decrease in the peak amplitude of the endotherm with $T_m \cong 47$ °C. The first and eighth scans are indicated by heavy solid and dotted lines, respectively. The inset shows excess heat capacity plots of the data after baseline subtraction for the first (heavy line), second (thin line), and eighth (dotted line) scans, where C_p is in the units kilocalories per kelvin per mole of monomer.

mg/mL), which is defective in autophosphorylation by PEP (*29*) and also dimerization (unpublished results), in the same buffer had T_m values of 45.4 and 54.8 °C at 30 °C/h. Corresponding Δ*H* values were 79 and 144 kcal/mol. These results suggest that the C-terminal domain of enzyme I is stabilized ∼5 °C and that the unfolding enthalpy is increased by higher ionic strength, whereas T_m and Δ*H* for N-terminal domain unfolding remained largely unaffected. Although no endotherms were observed on second DSC scans at the higher ionic strength and protein concentrations, it has been proposed that the system meets the criteria for microreversibility in that it is relatively insensitive to scan rate (*3*).

The last two entries in Table 2 are from measurements of thermally induced Trp exposure with the partially phosphorylated form of enzyme I isolated from the Δ*pts* strain (see Figure 6). The thermodynamic parameters obtained by fitting these data to a two-state model of unfolding were the same within experimental error as those obtained by fitting data for the dephospho form. In the presence of 2-ME, T_m was 41.1 ± 0.5 °C and van't Hoff Δ*H* was 58.4 ± 3.7 kcal/mol for either form of enzyme I. This indicates that the unfolding of the C-terminal domain, as reflected by Trp exposure, is independent of phosphorylation of His 189 in the N-terminal domain.

Eight consecutive DSC scans from 10 to 70 °C of partially phosphorylated enzyme I from the Δ*pts* strain, together with the buffer baseline, are shown in Figure 6. Excess heat capacity plots of the data from the first, second, and eighth scans were obtained after subtraction of the instrument baseline and normalization of the data (Figure 6, inset). The DSC results obtained with partially phosphorylated, intact enzyme I are similar to observations with partially phosphorylated EIN (Figure 1A). In both cases, repeated cycles of heating in the calorimeter resulted in the loss of a low-temperature endotherm and a corresponding increase in the amplitude of the high-temperature endotherm. Clearly, the amino-terminal domain in enzyme I is destabilized by phosphorylation. In addition, phosphorylation of enzyme I masked the endotherm with $T_m \cong 41$ °C produced by C-terminal domain unfolding (Figure 5A). Deconvolution of the first DSC scan in Figure 6 (inset) for multiple two-state transitions gave T_m values of 40.8, 47.1, and 54.0 °C with corresponding Δ*H* values of 58, 86, and 64 kcal/mol. Total areas after baseline subtraction were 210, 170, 160, and 120 kcal/mol for DSC scans 1, 2, 3, and 8, respectively, for the overall excess heat capacity. The endotherm due to C-terminal unfolding ($T_m \cong 41$ °C) was decreased ∼75% and was completely absent in the second and third DSC scans of Figure 6, respectively. Shifts in protein baselines and decreased areas probably were caused by irreversible denaturation of the C-terminal domain, which also affected the area of the high-temperature endotherm.

DISCUSSION

The endotherms observed with T_m values of 47 and 54 °C with partially phosphorylated enzyme I (Figure 6) are ∼3 °C lower than those observed with partially phosphorylated EIN (Figure 1A) in the same buffer. Thus, both phosphorylated and nonphosphorylated N-terminal domains in intact enzyme I appear to be energetically less stable than in the isolated EIN domain. These observations indicate that interactions between the N- and C-terminal domains of enzyme I occur (*28*), as proposed by LiCalsi et al. (*3*).

The measurements of unfolding enthalpies for EIN and enzyme I are not significantly affected by thermal hydrolysis of the phosphoryl group from phospho-His 189. The phosphotransfer potential of PEP (14.7 kcal/mol) is retained by phospho-enzyme I, which is phosphorylated at the $N^{\epsilon 2}$ position of His 189 (*30*). However, the hydrolysis of phospho-His 189 during DSC measurements would give a negative contribution of ∼1% to the overall positive unfolding enthalpy for EIN (140 kcal/mol) or for the amino terminal domain of intact enzyme I. In the experiment of Figure 1A, for example, initially ∼50% of EIN was phosphorylated (Figure 3) and ∼20% hydrolysis of phospho-His 189 occurred during each of five consecutive DSC scans, which amounts to ∼1.5 kcal/scan of heat released.

Phosphotransfer between EIN and HPr is reversible, but EIN is inactive in autophosphorylation by PEP (*3*, *7*). The C-terminal domain of enzyme I, which is linked to dimerization, is necessary for phosphorylation by PEP (*6*, *7*, *10*). The phosphorylation site (His 189) is buried in the EIN structure (*8*, *9*), whereas that of His 15 in HPr is solvent-exposed (*31*). The NMR solution structures of HPr have shown that phosphorylation of His 15 at the $N^{\delta 1}$ position produces only local structural perturbations (*32*, *33*). It is of interest to examine what structural features of the amino terminal domain of enzyme I might explain the 7 °C destabilization by phosphorylation that occurs without any loss in secondary structural elements contributing to the far-UV ellipticity.

The crystal structure of EIN (1−258 + Arg) determined by Liao et al. (*8*) showed that the protein has two distinct subdomains: one contains four α-helices arranged as two hairpins and the second consists of three- and four-stranded antiparallel and parallel β sheets, respectively, together with three short α-helices. The active-site His 189 is located at the junction of the two subdomains at the N-terminal end of Helix 6, which is connected to the third and fourth β strands. The $N^{\epsilon 2}$ atom of His 189 is hydrogen-bonded to the O^{γ} atom of Thr 168 in the adjacent helix 5 in a solvent-inaccessible environment. For phosphorylation to occur, the His 189 residue must rotate for exposure to phospho-HPr. Recent NMR studies of phosphorylated EIN (1−258 + Arg) have shown that this indeed occurs and that the pK_a of His 189 increases 1 pH unit. The most significant chemical shifts upon phosphorylation involve regions within the α/β domain and from Phe 65 to Glu 60 located at the interface between the α and α/β domains (*34*).

Parameters of energy functions in programs developed by Ernesto Freire and colleagues at the Biocalorimetry Center, The Johns Hopkins University (*35*), can predict ΔG to ±1 kcal/mol for folding/unfolding reactions of proteins (*36*−*38*). However, an error of only ±5% in the predicted entropy change results in an error of ± 15 °C in the predicted denaturation temperature, T_m (*39*).

A limitation in using structural information to predict thermodynamic parameters is illustrated in the thermal unfolding of nonphosphorylated and phosphorylated EIN. The reversible thermal unfolding of EIN is a two-state process, which means that there is a cooperative unfolding/refolding of the two subdomains without detectable intermediates. The cause of the 7 °C conformational destabilization that occurs on phosphorylation of EIN is not readily understood on the basis of structural information (or far-UV CD spectra). However, we can speculate that helix 1 and the loop structures at the beginning of the α subdomain in the structure of Liao et al. (*8*) are destabilized by phosphorylation of His 189 and that this has a corresponding destabilizing effect on adjacent helices 1, 2, and 3 without changing overall secondary structures at <40 °C. Also, it has been proposed by Meijberg et al. (*40*) that hydration of the phosphoryl group will lead to disruption of water structure and thus destabilization of the protein.

In summary, thermodynamic information (and especially T_m values) on the thermal unfolding of EIN are sensitive in detecting overall conformational perturbations produced by phosphorylation. In a related case, Huffine and Scholtz (*41*) replaced His 15 of HPr from *Bacillus subtilis* by the negatively charged glutamate to mimic phospho-His 15 and showed that this produced a significant decrease in the conformational stability of the protein, as measured by urea denaturation at 25 °C. His 15 of HPr is located at the N-terminus of the first helix and serves as a helix N-cap; the conformational stability of HPr with position 15 substitutions was observed to be Ala > His^0 > Glu^- > His^+ (*41*). Nevertheless, a NMR characterization of phosphorylated HPr from either *B. subtilis* or *E. coli* at position His 15 $N^{\delta 1}$ revealed only local structural perturbations, mainly in amide proton and nitrogen resonances of residues 16 and 17 (*32*). More recently, however, Van Nuland et al. (*33*), by using both NMR and molecular dynamics refinement, have detected a phosphorylation-induced torsion angle strain in the His 15 backbone of HPr that is released upon phosphoryl transfer.

Phosphotransfer is reversible because the high energy of phospho-His bonds is retained by the proteins of the PTS (*1*). The finding that HPr is destabilized by phosphorylation has led to the proposal that the conformational change promotes phosphotransfer to enzyme II (*33*). Our finding of a destabilization of enzyme I by phosphorylation supports and extends this idea, consistent with a phosphorylation−dephosphorylation cycle favoring unidirectional passage of phosphoryl groups from PEP to enzymes II and finally transport of available sugars across the membrane.

ACKNOWLEDGMENT

We are grateful to Dr. Henry M. Fales (LBC, NHLBI) for his help in analyzing and interpreting the mass spectral data reported here.

REFERENCES

1. Meadow, N. D., Fox, D. K., and Roseman, S. (1990) *Annu. Rev. Biochem. 59*, 497−542.
2. Postma, P. W., Lengeler, J. W., and Jacobson, G. R.(1996) in *Escherichia coli and Salmonella typhimurium*: *Cellular and Molecular Biology* (Neidhardt, F. C., Ed.) pp 1149−1174, American Society for Microbiology Press, Washington, DC.
3. LiCalsi, C., Crocenzi, T. S., Freire, E., and Roseman, S. (1991) *J. Biol. Chem. 266*, 19519−19527.
4. Han, M. K., Roseman, S., and Brand, L. (1990) *J. Biol. Chem. 265*, 1985−1995.
5. Lee, B. R., Lecchi, P., Pannell, L., Jaffe, H., and Peterkofsky, A. (1994) *Arch. Biochem. Biophys. 312*, 121−124.
6. Chauvin, F., Brand, L., and Roseman, S. (1996) *Res. Microbiol. 147*, 471−479.
7. Seok, Y.-J., Lee, B. R., Zhu, P.-P., and Peterkofsky, A. (1996) *Proc. Natl. Acad. Sci. U.S.A. 93*, 347−351.
8. Liao, D.-I., Silverton, E., Seok, Y.-J., Lee, B. R., Peterkofsky, A., and Davies, D. R. (1996) *Structure 4*, 861−872.
9. Garrett, D. S., Seok, Y.-J., Liao, D.-l., Peterkofsky, A., Gronenborn, A. M., and Clore, G. M. (1997) *Biochemistry 36*, 2517−2530.
10. Chauvin, F,. Fomenkov, A., Johnson, C. R., and Roseman, S. (1996) *Proc. Natl. Acad. Sci. U.S.A. 93*, 7028−7031.
11. LaVallie, E. R., DiBlasio, E. A., Kovacic, S., Grant, K. L., Schendel, P. F., and McCoy, J. M. (1993) *Bio/Technology 11*, 187−193.
12. Miller, J. H. (1972) *Experiments in Molecular Genetics*, Cold Spring Harbor Laboratory Press, Cold Spring Harbor, NY.
13. Levy, S., Zeng, G.-Q., and Danchin, A. (1990) Gene *86*, 27−33.
14. Reddy, P., Fredd-Kuldell, N., Liberman, E., and Peterkofsky, A. (1991) *Protein Expression Purif. 2*, 179−187.
15. Laemmli, U. K. (1970) *Nature (London) 227*, 680−685.
16. Waygood, E. B. (1986) *Biochemistry 25*, 4085−4090.
17. Yang, J. T., Wu, C. S., and Martinez, H. M. (1986) *Methods Enzymol. 130*, 208−269.
18. Kirchhoff, W. H. (1993) *NIST Technical Note 1401*: *EXAM* (CODEN: NTNOEF), U.S. Government Printing Office, Washington, DC.
19. Plotnikov, V. V., Brandts, J. M., Lin, L.-N., and Brandts, J. F. (1997) *Anal. Biochem. 250*, 237−244.
20. Privalov, G., Kavina, V., Freire, E., and Privalov, P. L. (1995) *Anal. Biochem. 232*, 79−85.
21. Ginsburg, A., and Zolkiewski, M. (1991) *Biochemistry 30*, 9421−9429.
22. Waygood, E. B., and Steeves, T. (1980) *Can. J. Biochem. 58*, 40−48.
23. Zamyatnin, A. (1984) *Annu. Rev. Biophys. Bioeng. 13*, 145−165.
24. Maurizi, M. R., Pinkofsky, H. B., McFarland, P. J., and Ginsburg, A. (1986) *Arch. Biochem. Biophys. 246*, 494−500.

25. Wu, Q., Liu, C., and Smith, R. D. (1996) *Rapid Commun. Mass Spectrom. 10*, 835−838.
26. Privalov, P. L. (1979) *Adv. Protein Chem. 33*, 167−241.
27. Chauvin, F., Brand, L., and Roseman, S. (1994) *J. Biol. Chem. 269*, 20263−20269.
28. Brandts, J. F., Hu, C. Q., Lin, L. N., and Mas, M. T. (1989) *Biochemistry 28*, 8588−8596.
29. Seok, Y.-J., Lee, B. R., Gazdar, C., Svenson, I., Yadla, N., and Peterkofsky, A. (1996) *Biochemistry 35*, 236−242.
30. Weigel, N., Kukuruzinska, A., Nakazawa, A., Waygood, E. B., and Roseman, S. (1982) *J. Biol. Chem. 257*, 14477−14491.
31. Herzberg, O., and Klevit, R. (1994) *Curr. Opin. Struct. Biol. 4*, 814−822.
32. Rajagopal, P., Waygood, E. B., and Klevit, R. E. (1994) *Biochemistry 33*, 15271- 15282.
33. Van Nuland, N. A. J., Wiersma, J. A., Van der Spoel, D., De Groot, B. L., Scheek, R. M., and Robillard, G. T. (1996) *Protein Sci. 5*, 442−446.
34. Garrett, D. S., Seok, Y.-J., Peterkofsky, A., Clore, G. M., and Gronenborn, A. M. (1998) *Protein Sci. 7*, 789−793.
35. Murphy, K. P., and Freire, E. (1992) *Adv. Protein Chem. 43*, 313−361.
36. Gómez, J., Hilser, V. J., Xie, D., and Freire, E. (1995) *Proteins*: *Struct. Funct., Genet. 22*, 404−412.
37. Hilser, V. J., Gómez, J., and Freire, E. (1996) *Proteins*: *Struct., Funct., Genet. 26*, 123−133.
38. Hilser, V. J., Townsend, B. D., and Freire, E. (1997) *Biophys. Chem. 64*, 69−79.
39. D'Aquino, J. A., Gómez, J., Hilser, V. J., Lee, K. H., Amzel, L. M., and Freire, E. (1996) *Proteins*: *Struct., Funct., Genet. 25*, 143−156.
40. Meijberg, W., Schuurman-Wolters, G. K., and Robillard, G. T. (1996) *Biochemistry 35*, 2759−2766.
41. Huffine, M. E., and Scholtz, J. M. (1996) *J. Biol. Chem. 271*, 28898−28902.

BI980126X